

Selective Synthesis of Dimethylamine over Small-Pore Zeolites: Catalytic Selectivity and Sorption Behavior

LLOYD ABRAMS, MICHAEL KEANE, JR., AND GEORGE C. SONNICHSEN

Central Research & Development Department,¹ E. I. du Pont de Nemours & Company, Experimental Station, Wilmington, Delaware 19880-0262

Received July 12, 1988; revised September 26, 1988

Sorption measurements of alcohols were used to rationalize the performance of zeolites used as catalysts for the synthesis of methylamines via the sequential reaction of methanol and ammonia. Low methanol absorption corresponds to low catalytic activity while high isopropanol absorption corresponds to zeolites producing an equilibrium distribution of methylamines. Generally, zeolites, with sorption values for methanol (or ethanol) of 10-30 w/o and little or no isopropanol sorption, selectively produce mono- and dimethylamines versus trimethylamine. Mineral chabazites, while having similar activities, surprisingly provide a wide range of product selectivities. The Geometric Selectivity Index, GSI, defined as the ratio of methanol sorption to the sorption of *n*-propanol, was found to correspond to the observed catalytic selectivity of the mineral chabazites. © 1989 Academic Press, Inc.

INTRODUCTION

Mono-, di-, and trimethylamines are made commercially by the exothermic reaction of methanol and ammonia over solid acid catalysts (1). The reaction proceeds toward a thermodynamically predictable distribution of the three amines which favors the production of trimethylamine, TMA. At 99% conversion of methanol, the equilibrium product distribution is 27/23/50 (mol%) for mono-/di-/trimethylamines, respectively. However, the greatest market demand is for dimethylamine, DMA (2). Catalysts with selectivities toward a methylamine product distribution matching the market demand (33/53/14) (2) are the goal of this work.

Earlier work showed that zeolites are selective catalysts for the formation of mono- and dialkylamines from alcohols, ethanol and butanol, and ammonia (3). Using methanol as the alcohol source, Weigert demonstrated selectivity toward monomethylamine (MMA) and DMA over a sodium

mordenite catalyst (4). Selectivities over this catalyst were $MMA > DMA > TMA$ and Weigert attributed sorption selectivity to be critical in determining the catalysts' selectivity. However, in terms of size, $MMA < DMA < TMA$, so that the product distribution is inversely related to the increasing size of the amine products and suggests that the mordenite catalyst selectivity is based on size.

As noted above, dimethylamine is the desired product. Weigert's success in finding a catalyst with a nonequilibrium product distribution prompted us to examine other zeolites for further improvements in selectivity to DMA as well as activity. As such, a variety of catalysts was examined to develop a rational basis for enhanced DMA selectivity (5). However, extensive catalyst characterization using techniques such as X-ray and neutron diffraction, IR and NMR spectroscopies, were unable to demonstrate a direct correlation to the observed catalytic selectivity (6).

The apparent relationship in Weigert's experiments of product distribution to molecular size prompted us to examine the

¹ Contribution No. 4807.

catalytic data in terms of the sorption properties of the catalysts. Catalytic data, in the form of product distribution versus percentage methanol converted, provide a direct measure of reaction selectivity. Furthermore, reactor operation was sufficiently reliable and reproducible such that product distribution data could be used to characterize catalysts. Product distribution versus reactant conversion data were fitted using the GEAR iteration program, HAVCHEM (7), modified for use on a Digital VAX 8600 to calculate relative rate constants for the reaction steps involved. In his paper, Weigert provides several examples of conventional catalytic data (in the form of molar selectivity vs methanol conversion) that were fit using the HAVCHEM program (4). The calculated rate constants provide a quantitative description of selectivity for a given catalyst. These rate constants were then compared to sorption data for various catalysts to provide a rational basis for the selectivities observed in the methylamine synthesis from methanol and ammonia.

EXPERIMENTAL

Samples of chabazite zeolites were obtained from various mines and X-ray diffraction analysis showed that chabazite was the predominant phase (traces of erionite were present in some samples). Two amorphous aluminosilicates were examined: a laboratory-prepared material with a 1:3 Al_2O_3 : SiO_2 ratio and a commercial sample of ~95% alumina, Al-1602, obtained from the Harshaw Co. A variety of other zeolites (see text) was obtained or synthesized and examined as catalysts. Catalyst handling was previously described (6).

The reactor, a $\frac{1}{4}$ × 12-in. stainless-steel U-tube with an internal diameter of 0.215 in., was loaded with 0.5 to 2.0 g of sieved catalyst. Feed rate was controlled by an ISCO syringe pump. A premixed liquid with a molar composition of 1:1 methanol to ammonia was pumped through a Grove

diaphragm regulator set at a backpressure of 300 psig. Pressure was reduced to atmospheric and the mix was vaporized and heated to 200°C before contacting the catalyst.

The reactor was immersed in a nitrogen fluidized sand bath. Reactor temperature was controlled by an Athena temperature controller. Heat was supplied by a resistance coil just above the nitrogen sparger. Thermocouples, attached to the exterior U-tube walls, indicated an approximate catalyst temperature.

Feed rate and reactor temperature were varied to obtain as wide a range of reactant conversion as possible. Molar concentrations of products and reactants in the reactor effluent were measured at 95°C by a GOW/MAC Series 550 gas chromatograph. The chromatograph column was an $\frac{1}{8}$ × 18-in. precolumn of 20% Carbowax 400 treated with 2.5% KOH on Chromosorb NAW and an $\frac{1}{8}$ × 144-in. column of 4% Carbowax 20M/0.8% KOH on Carbowax B (Supelco 1-1887).

Reactants were not fed to the reactor until it was heated to 200°C (approximately $\frac{1}{2}$ h from 25°C). This ensures that reactants and products are vapors. A series of four to six chromatograms was taken under each condition to ensure that reactor operation was lined out. No deterioration in catalytic performance was observed during the time frame of a scouting run, typically 6 h long. Chromatograms were stored on a computer database.

Sorption measurements were made using a vacuum-tight apparatus similar to that described by Landolt (8). The apparatus was divided into two sections: an adsorption manifold and a vacuum outgassing station with a programmed temperature ramping controller. Twenty-four samples were treated simultaneously on each section. A sample holder employing a greaseless vacuum stopcock and an O-ring seal was designed to contain the samples and fit on an analytical balance. Sample handling procedures provide a reproducibility of 0.6% for

samples sorbing 100 mg per gram of sample.

Typically, 0.5–1 g of zeolite was pressed at 500–5000 psi into self-supporting cylinders and placed into a preweighed sample holder. The holders were attached to the vacuum manifold and pumped out. Heating was done under vacuum with a programmed temperature ramping of 30–70°C/h to 425°C. At 425°C, the samples were exposed to oxygen at 100–300 Torr (1 Torr = 133.3 N m⁻²) to assist in the removal of residual organics. The oxygen was pumped off until the pressure above the samples was $<2 \times 10^{-5}$ Torr. At that point, the outgassing rate was measured by turning off the main vacuum valve; if the outgassing rate was <0.1 mTorr/min at 425°C, the samples were then cooled under vacuum and weighed. If the outgassing rate was higher, then heating under vacuum at 425°C was continued. The outgassing procedure generally takes 16–50 h to reach 2×10^{-5} Torr depending upon the sorbate being removed and the pore size of the zeolites. The weight of powder dried in this fashion was used to calculate the amount sorbed per gram of sample. Note that if the outgassing criterion was not met, sorption weights 10–25% low were measured and sorption rates were not reproducible.

After the outgassed samples were weighed, they were mounted onto the sorption manifold. The samples were then exposed at room temperature to a solvent vapor at 0.1–0.5 of its vapor pressure at that temperature. Doing so reduced the contribution of multilayer adsorption on the exterior particle surface of the samples and eliminated condensation on the manifold and sample holder walls. Samples could be removed from the sorption manifold at any time during the sorption process and the weight gain recorded. Typically, weighings at 3 and 20 h were taken. When the sorption process was slow or the weight gain negligible, the duration of exposure was increased. Generally, the same samples were used for a series of adsorption and desorp-

tion experiments. Sample weights were checked after heating under vacuum at 425°C and, if warranted, the samples were returned to the desorption rack for an oxygen treatment.

High-purity solvents were vacuum distilled, subjected to several freeze–thaw cycles, and stored over dry zeolite 4A in a bulb with a greaseless vacuum stopcock. The liquids used for this study were methanol (MeOH), ethanol, *n*-propanol (*n*PrOH), and *i*-propanol (*i*PrOH). Since the catalytic reaction occurs at 400°C and the sorption process is studied at 25°C, it was essential to find molecules that could mimic the migration behavior of TMA at the reaction temperature. By following the tedious desorption procedures, fouling of the zeolites was minimal and the same samples could be used for a variety of solvent exposures. Sorption of alcohols at temperatures much higher than 25°C would provide ambiguous results because they catalytically dehydrate. However, mono-, di-, and trimethylamines strongly chemisorb to the zeolite frameworks, pyrolyze during the desorption process, and leave a residue in the framework thereby requiring a new sample for each experiment.

Adsorption (External Surface) vs Absorption (Internal Framework)

The measured weight gain for a sample is distributed among external surface adsorption and internal framework absorption processes. For small zeolite particles, the external surface may contribute significantly to the total amount sorbed (adsorption) and a method to distinguish this amount from that absorbed into the framework was developed.

One of the cells of a given series of 24 samples contained a nonmicroporous amorphous aluminosilicate with a BET surface area of 102 m²/g. Under the experimental sorption conditions, the amount of solvent adsorbed by this material was used to determine the external surface coverage, *k*. For molecules too large to enter the zeolite

framework, the weight pickup by a sample, W , should equal the product of the external surface area, SA, and k , that is, $W = k \times SA$ providing the external surface of the zeolite is nonmicroporous. For a physical adsorption process of the same solvent molecule on surfaces of similar chemistry at the same temperature, this relationship should be valid.

In order to make the correction for the amount adsorbed, a measure (other than adsorption) of external surface area is needed especially when there is a significant amount of absorption. Mercury porosimetry measurements and calculations based on them were used to obtain the exterior surface areas of these zeolites. Porosimetry data were obtained to 60 kpsi using a Micrometrics Model 9200 autopore. The data output is the mercury intrusion volume as a function of applied pressure. The radius of a pore, r , is related to the applied pressure, P , via the Washburn equation, $r = -2\sigma \cos(\theta)/P$, where σ is the surface tension and θ is the contact angle. For the present study, a contact angle of 130° and surface tension of 485 dyn/cm were used. For the pressure range of study, 0–60 kpsi, mercury could not penetrate into the zeolite pores. Once the corresponding pressure–intrusion volume data were obtained, the incremental surface area contribution for each intrusion volume was calculated and then summed up to provide an estimate of the external surface area of a sample.

For soft materials such as silicates, compression and/or comminution of the particles may occur by the high pressures of the porosimetry measurement. For samples which show smooth exterior surfaces via SEM, large increases in the calculated Hg surface areas with increasing pressure signal this problem. For many of the zeolites, large increases in Hg porosimetry areas were observed at 50–60 kpsi.

Sorption experiments were conducted on different small-pore zeolites with nonmicroporous external surfaces using solvent molecules too large to enter the framework,

for example, benzene, neopentane, isopropanol, *p*-xylene. External surface areas for these zeolites were calculated from the sorption data by ratioing the amount adsorbed by these samples to the amount adsorbed by the control sample (102 m²/g) under identical conditions of temperature and pressure. The surface areas calculated from Hg porosimetry data at 45 kpsi were then compared to the surface areas obtained from the adsorption experiments as shown in Fig. 1. The surface areas from the two methods were found to agree within 5% if the samples did not have appreciable micropores.

The surface area obtained from mercury porosimetry could then be used to calculate the weight gain contributed by the adsorbed molecules on the surface of zeolite particles, W_a , via the equation $W_a = k \times SA$. At any time during an experiment, the total weight gain by a sample, W_t , comprises this surface adsorbed contribution (W_a) and the framework absorbed amount, W_f , such that $W_t = W_a + W_f$. The amount absorbed into the framework, W_f , is obtained by subtracting the surface contribution from the total weight gain, $W_f = W_t - W_a$. Values reported in this paper, unless stated otherwise, have been corrected in this manner. Most of the external surface areas of the zeolites were in the range 10–40 m²/g and accounted for 2–5% of the total amount sorbed.

RESULTS AND DISCUSSION

A reaction mechanism, based on the stepwise addition of methanol to ammonia, describes the formation of methylamines via steps 1, 2, and 3 as shown in Table 1. While water and the methylamines are the primary products, varying amounts of dimethyl ether, DME, may also be produced. The observed product distribution depends on the extent of conversion (Table 2) of the primary reactants, MeOH and NH₃, as previously reported (5, 6). However, rate constants, because they are valid descriptors

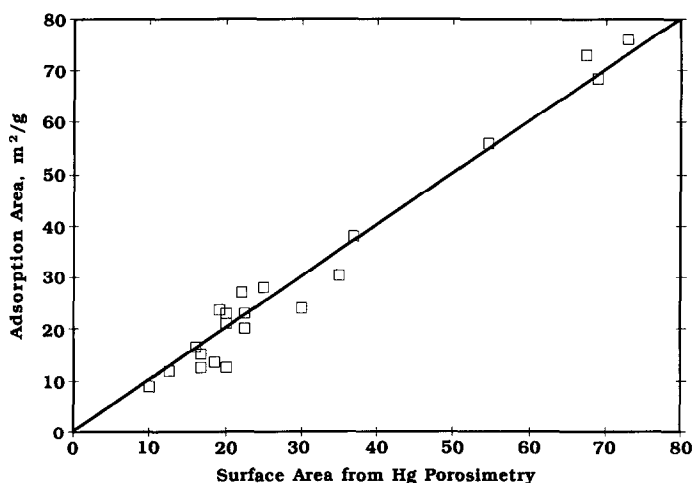


FIG. 1. Comparison of surface areas calculated from mercury porosimetry (to 45 kpsi) to the surface areas obtained from adsorption measurements.

over the entire range of conversion, were used to compare catalyst performance instead of selectivity at a specific conversion. The thrust of our program is to produce DMA while eliminating or limiting the amount of TMA in the product stream. As such, we devised a figure of merit, a ratio of the rate constants, k_2/k_3 , which describes the rate of DMA formation relative to its consumption to make TMA. Therefore, catalysts with a high selectivity toward

DMA should have a higher k_2/k_3 ratio than unselective catalysts which produce an equilibrium product distribution.

Thermodynamically driven reactions, if allowed to proceed, will provide an equilibrium product distribution. Indeed, the products over amorphous silica-alumina catalysts approach the equilibrium distribution ratio as shown in Table 3. The k_2/k_3 ratio is significantly less than one demonstrating the lack of constraints on the conversion of DMA to TMA. Dehydration of methanol to the by-product dimethyl ether also occurs in competition with the amine synthesis reactions. The rate constant for producing DME from methanol depends on

TABLE 1

Reaction Pathway (Steps 1-3) for the Formation of Methylamines from Ammonia, NH_3 , and Methanol, MeOH , over Silica-Aluminas (The Parallel Reaction (4) to Make Dimethyl Ether, DME, Is Also Shown)

		ΔG° (kcal/g mol)
$\text{NH}_3 + \text{MeOH} \xrightarrow{k_1} \text{MMA} + \text{H}_2\text{O}$	(1)	-4.3
$\text{MMA} + \text{MeOH} \xrightarrow{k_2} \text{DMA} + \text{H}_2\text{O}$	(2)	-7.3
$\text{DMA} + \text{MeOH} \xrightarrow{k_3} \text{TMA} + \text{H}_2\text{O}$	(3)	-8.6
$2\text{MeOH} \xrightarrow{k_4} \text{DME} + \text{H}_2\text{O}$	(4)	-4.2
Other reactions that contribute to the product stream (generally at MeOH conversions >90%)		
$2\text{MMA} \rightarrow \text{DMA} + \text{NH}_3$	(5)	
$2\text{DMA} \rightarrow \text{TMA} + \text{MMA}$	(6)	
$\text{NH}_3 + \text{DME} \rightarrow \text{MMA} + \text{MeOH}$	(7)	

TABLE 2

Activity of a Typical Sample (Naples Chabazite)

Temperature (K)	Space velocity (h^{-1})	Methanol conversion (%)
623	0.5	8
	0.25	82
673	3	61
	2	75
	1	87
	1	92
	0.5	98

TABLE 3
Product Distributions over Amorphous Silica-Alumina Catalysts

	Catalytic selectivity ^a				Rate constant ratios			
	MMA	DMA	TMA	DME	k_2/k_1	k_3/k_1	k_4/k_1	k_2/k_3
3:1 Silica:alumina ratio	14	13	49	24	22.8	42.1	1.35	0.54
Harshaw Al-1602	21	11	34	34	8.5	11.8	6.3	0.72
Equilibrium	17	21	62					

^a Molar selectivity at 90% MeOH conversion.

the alumina content of the catalyst; the more alumina, the higher the k_4/k_1 ratio. The difference in k_2/k_3 ratios for the two silica-alumina catalysts is not really significant in terms of shifting the methylamine product distribution from the equilibrium values. If, however, the conversion of DMA to TMA (step 3) could be sterically or chemically inhibited without greatly affecting the conversion of DMA, then the product stream should be richer in dimethylamine. This is equivalent to raising the k_2/k_3 ratio significantly above unity.

Shown in Table 4 are the catalytic and sorption data for zeolites of different pore sizes. These zeolites yield product streams rich in TMA with k_2/k_3 ratios close to those observed for the nonselective silica-aluminas in Table 3. Isopropanol sorption clearly identifies the reason for the lack of inhibi-

tion of the DMA → TMA conversion reaction. Each of the zeolites noted in Table 4 (except ferrierite) absorbs a significant amount of *i*PrOH at room temperature. An *i*PrOH molecule is very close to the size and shape of a TMA molecule and indicates that TMA produced within the framework (via step 3) should have little or no hindrance in exiting from the zeolite framework and entering the product stream. Apparently, isopropanol (and TMA by analogy) can pass readily through 12-, 10-, and 8-membered ring systems that form the intracrystalline channels within the zeolites' frameworks. These experiments demonstrate that zeolites with an *i*PrOH sorption of >3 g/100 g are not catalytically selective toward DMA and yield product distributions close to the equilibrium values.

TABLE 4
Data for Various Zeolites Used as Methylamine Catalysts

Zeolite	Catalytic selectivity ^a				k_2/k_3	Pore size ^b	Sorption data ^c	
	MMA	DMA	TMA	DME			MeOH	<i>i</i> PrOH
H-Y	12	11	61	16	0.52	12	25.3	21.9
H-mordenite (large pore)	18	13	68	1	0.59	12	14.0	8.9
H-ZSM-5	3	7	67	22	0.04	10	14.0	12.7
H-Ferrierite	31	27	36	7	0.53	10,8	7.2	0.2
Ca-A	25	20	50	7	0.64	8	21.7	5.6

^a Molar selectivity at 90% MeOH conversion.

^b Number of T-O bonds forming continuous channels.

^c Grams absorbed of solvent (methanol, isopropanol) per 100 g dry sample at 20–25°C, 20 h.

TABLE 5
Relatively Inactive Zeolites

Zeolite	Reaction temperature (°C)	% MeOH conversion ^a	Pore size ^b	Sorption data ^c	
				MeOH	<i>i</i> PrOH
Brewsterite	400	4	8	0.0	0.0
Edingtonite	400	23	8	0.8	0.5
Analcime	400	4	6	0.3	0.1
Natrolite	400	4	8	0.3	0.1
P	400	15	8	0.5	0.2
Gmelinite	400	6	8	8.9	2.0

^a Very long reactor contact times were needed to realize these modest conversions.

^b Number of T-O bonds forming continuous channels.

^c Grams absorbed of solvent per 100 g dry sample at 20–25°C, 20 hr.

Mordenite possesses channels with different numbers of T-O members in the rings: a 12-membered one and an 8-membered one. X-ray diffraction of the zeolite does not readily distinguish which of the two channel systems is controlling the catalytic or sorption processes. For the sample noted in Table 4, the sorption value of *i*PrOH indicates that the pores are accessible for absorption, hence, the designation large-pore mordenite. For this zeolite, TMA is readily released from the framework into the product stream thereby yielding close to the equilibrium distribution. Ferrierite, however, displays a very low *i*PrOH amount sorbed such that the 10- and 8-membered rings must be partially blocked. Indeed, the low methanol sorption value indicates that absorption of one of the reactant molecules to the framework is also hindered. In this case, the catalytic reaction on the surface of the ferrierite particles dominates the product distribution and is similar in selectivity to the amorphous silica-aluminas.

The sorption of *i*PrOH could now be used as a gauge to indicate which zeolites would produce near-equilibrium product distributions. Table 5 shows the results for catalysts that have low (or no) *i*PrOH sorption. Furthermore, the external surface areas of these zeolites were also very low

such that reactions on their surfaces might be a minor contributor to the product distribution. But the methanol sorption of these zeolites is also very low. Thus, methanol, one of the reactants in the methylamine synthesis, cannot sorb into the framework to react and the resulting low catalytic activity reflects this fact. Very long contact times in the reactor were required to achieve the modest conversions noted in Table 5. The product streams were very rich in MMA with little, or no TMA, but the range of reactant conversion was insufficient to permit calculation of k_2/k_3 values.

Thus, zeolites, with channels composed of 10- or 12-membered T-O rings, are large enough to permit *i*PrOH to readily absorb (and therefore to permit TMA to exit into the product stream) and are not selective. Small-pore zeolites, 6-membered T-O rings, do not permit rapid transfer of the reactants into the framework such that they are virtually inactive under the reactor conditions used. On the basis of the trade-off of the effects of ring members, our efforts focused on the catalytic selectivity of various 8-ring zeolites. As shown in Table 6, some 8-ring zeolites provide a product distribution richer in mono- and dimethylamines than that obtained via the equilibrated system, that is, $k_2/k_3 > 0.8$. The low value of *i*PrOH sorption for the mordenite sample

TABLE 6
Data for Zeolites with $k_2/k_3 > 0.8$

Zeolite	Catalytic selectivity ^a				k_2/k_3	Pore size ^b	Sorption data ^c	
	MMA	DMA	TMA	DME			MeOH	<i>i</i> PrOH
Chabazite (Bowie)	12	22	63	3	0.9	8	13.9	0.1
H-mordenite (small pore)	37	33	26	4	1.2	8	14.0	1.6
H-erionite	32	19	13	36	1.6	8	10.1	0.1
Chabazite (Durkee)	20	43	32	5	3.4	8	16.8	0.05

^a Molar selectivity at 90% MeOH conversion.

^b Number of T-O bonds forming continuous channels.

^c Grams absorbed of solvent (methanol, isopropanol) per 100 g dry sample at 20–25°C, 20 h.

showed that the small-pore system was controlling both the sorption and the catalytic processes. Somewhat fortuitously, two samples of chabazite were used as catalysts and they provided significantly different product distributions. Other than the fact that the chabazite samples came from two different locations, there was no apparent reason for the surprising difference in catalytic selectivities. X-ray diffraction patterns for the two samples are almost identical with very little, if any, of other phases present. The sorption data of MeOH and *i*PrOH certainly did not distinguish the samples from each other. An intermediate-sized molecule, *n*PrOH, was then used to

characterize these and other chabazite samples to determine if there are differences in sorption behavior which could explain the observed differences in catalytic selectivity.

Shown in Table 7 are the sorption and catalytic data for a variety of chabazite zeolites identified by the location of their mine. Again, X-ray diffraction measurements on these samples showed them to be virtually identical. Sorptions of ethyl and *n*-propyl alcohols were used to determine if they would readily distinguish these zeolites. Ethanol sorption data were virtually identical to the methanol data but *n*-PrOH values were different for the samples. Sorption

TABLE 7
Data for Chabazite Zeolites

Mine location	Catalytic selectivity ^a				k_2/k_3	Sorption data ^b			
	MMA	DMA	TMA	DME		MeOH	<i>n</i> PrOH	<i>i</i> PrOH	GSI ^c
Bowie, Arizona	12	22	63	3	0.9	13.9	10.6	0.1	1.3
Bear Springs, Arizona	14	26	59	2	1.2	11.1	8.3	0.07	1.3
Wikieup, Arizona	16	29	53	2	1.2	13.0	9.3	0.07	1.4
Christmas, Arizona	15	32	50	4	1.4	17.6	6.5	0.02	2.7
Beaver Divide, Wyoming	18	33	48	1	1.4	11.3	3.9	0.02	2.9
Durkee, Oregon	20	43	32	5	3.4	16.8	4.4	0.05	3.8
Nova Scotia, Canada	18	42	40	0	4.6	20.8	4.8	0.01	4.3
Naples, Italy	25	60	15	1	6.2	13.3	2.5	0.02	5.3

^a Molar selectivity at 90% MeOH conversion.

^b Grams absorbed of solvent per 100 g dry sample at 20–25°C, 20 h.

^c GSI is defined as the net sorption of methanol (20 h) divided by the net sorption of *n*-propanol (20 h).

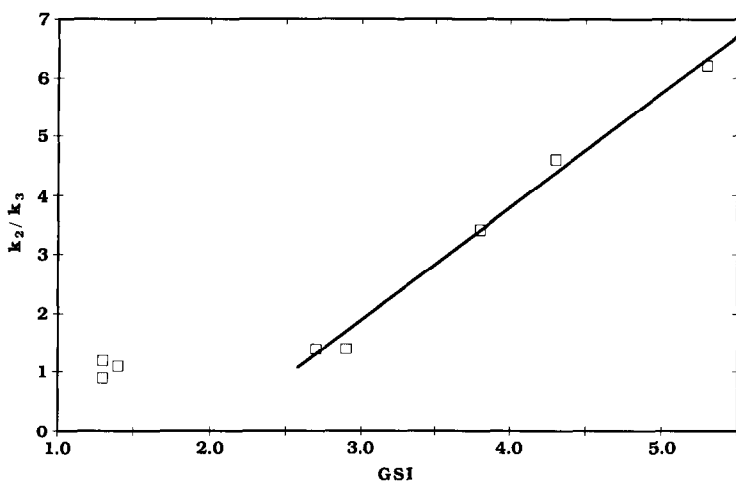


FIG. 2. Relationship of GSI (the ratio of the absorption amounts of methanol to *n*-propanol) to the methylamine catalytic selectivity (expressed as the ratio of rate constants to make DMA and TMA).

measurements, based on a combination of the MeOH and *n*PrOH data, readily distinguish the mineral chabazites from one another. The Geometric Selectivity Index, GSI, was defined as the ratio of MeOH sorbed in 20 h to *n*-PrOH sorbed in 20 h. The GSI shows that one mineral chabazite may be significantly different from another mineral chabazite and these differences in sorption behavior could not be predicted beforehand. The sorption value of MeOH essentially indicates how much of the framework is accessible for absorption and the catalytic process. The sorption of the somewhat geometrically larger molecule, *n*PrOH, shows that some constraints are present. In the absence of constraints, the *n*PrOH sorption value would be virtually equal to the MeOH value, that is, GSI = 1.

Ordering the mineral chabazites in terms of increasing GSI provides a ranking for their selectivity performance as catalysts, in terms of k_2/k_3 , in the methanol/ammonia reaction; this relationship is shown in Fig. 2. Thus, when GSI \sim 1–2.5, *n*PrOH and MeOH occupy the same framework volume and enter and leave the framework fairly readily. When the GSI $>$ 3, the migration of *n*-PrOH is hindered within the zeolite framework; longer sorption times yield

higher sorption values. Using the same time limit for all *n*-PrOH sorption (20 h) in effect provides a measure of migration or diffusion within the frameworks. The sorption of *n*-propanol is hindered to varying degrees within the chabazites and it is this behavior that mimics the sorption/migration behavior of TMA from the chabazite framework into the product stream. The fact that there is a strong correspondence between GSI and DMA yield also indicates that reactions on the chabazite particles' exterior surfaces do not contribute substantially to the observed product distribution.

CONCLUSIONS

The selectivity of zeolite catalysts for the synthesis of methylamines was able to be rationalized on the basis of absorption measurements of alcohols at 25°C. For example, low methanol absorption (3–5 w/o) corresponds to low catalytic activity. Isopropanol, because it is very similar to TMA in size and shape, was used as a gauge to indicate whether TMA could readily exit from a zeolite framework. When the framework restricts TMA migration without greatly affecting DMA egress to the reactor effluent, a catalyst may exhibit DMA selectivity. Isopropanol sorption $>$ 3 w/o

corresponds to zeolites producing almost an equilibrium distribution of methylamines. Generally, zeolites, with sorption values for methanol (or ethanol) of 10–30 w/o and little or no isopropanol sorption, selectively produce MMA and DMA versus TMA.

Mineral chabazites, while having similar activities, surprisingly provide a wide range of product selectivities. The GSI was defined as the ratio of methanol sorption to the sorption of *n*-propanol. Methanol provides a measure of framework capacity, while *n*-propanol mimics the migration behavior of TMA from the framework of the chabazites into the reactor product stream. For the variety of chabazite minerals studied, an increase in GSI was found to correspond to an increase in DMA selectivity.

REFERENCES

1. *Hydrocarbon Process.* **58**, 195 (1979).
2. "Riegel's Handbook of Industrial Chemistry" (J. A. Kent, Ed.), 8th ed., p. 187. Van Nostrand-Reinhold, Princeton, NJ, 1983.
3. Hamilton, L. A., U.S. Patent 3,384,667 (1968).
4. Weigert, F. J., *J. Catal.* **103**, 20 (1987). Rate Constants, reported here, calculated according to Weigert's Method had standard deviations of about 5%.
5. Keane, M., Jr., Sonnichsen, G. C., Abrams, L., Corbin, D. R., Gier, T. E., and Shannon, R. D., *Appl. Catal.* **32**, 361 (1987).
6. Shannon, R. D., Keane, M., Jr., Abrams, L., Stabler, R. H., Gier, T. E., Corbin, D. R., and Sonnichsen, G. C., *J. Catal.* **113**, 367 (1988); **114**, 8 (1988); **115**, in press. Note that these papers provide extensive characterization of the zeolites used in this study.
7. Stabler, R. N., and Chesnick, J., *Int. J. Chem. Kinet.* **10**, 461 (1978).
8. Landolt, G. R., *Anal. Chem.* **43**, 613 (1971).